Chapter 19
The Pyruvate Dehydrogenase Complex and Related Assemblies in Health and Disease

Olwyn Byron and John Gordon Lindsay

Abstract The family of 2-oxoacid dehydrogenase complexes (2-OADC), typified by the pyruvate dehydrogenase multi-enzyme complex (PDC) as its most prominent member, are massive molecular machines (M_r, 4–10 million) controlling key steps in glucose homeostasis (PDC), citric acid cycle flux (OGDC, 2-oxoglutarate dehydrogenase) and the metabolism of the branched-chain amino acids, leucine, isoleucine and valine (BCOADC, branched-chain 2-OADC). These highly organised mitochondrial arrays, composed of multiple copies of three separate enzymes, have been widely studied as paradigms for the analysis of enzyme cooperativity, substrate channelling, protein-protein interactions and the regulation of activity by phosphorylation. This chapter will highlight recent advances in our understanding of the structure-function relationships, the overall organisation and the transport and assembly of PDC in particular, focussing on both native and recombinant forms of the complex and their individual components or constituent domains. Biophysical approaches, including X-ray crystallography (MX), nuclear magnetic resonance spectroscopy (NMR), cryo-EM imaging, analytical ultracentrifugation (AUC) and small angle X-ray and neutron scattering (SAXS and SANS), have all contributed significant new information on PDC subunit organisation, stoichiometry, regulatory mechanisms and mode of assembly. Moreover, the recognition of specific genetic defects linked to PDC deficiency, in combination with the ability to analyse recombinant PDCs housing both novel naturally-occurring and engineered mutations, have all stimulated renewed interest in these classical metabolic assemblies. In addition, the role played by PDC, and its constituent proteins, in certain disease states will be briefly reviewed, focussing on the development of new and exciting areas of medical and immunological research.

O. Byron
School of Life Sciences, University of Glasgow, Glasgow G12 8QQ, UK
e-mail: Olwyn.Byron@glasgow.ac.uk

J.G. Lindsay (✉)
Institute of Molecular, Cell and Systems Biology, Davidson Building, College of Medicine, Veterinary and Life Sciences, University of Glasgow, Glasgow G12 8QQ, UK
e-mail: Gordon.Lindsay@glasgow.ac.uk

J.R. Harris, J. Marles-Wright (eds.), *Macromolecular Protein Complexes*,
Subcellular Biochemistry 83, DOI 10.1007/978-3-319-46503-6_19

Keywords Pyruvate dehydrogenase complex • Reaction cycle • Supramolecular architecture • Structure-function relationship • Biophysical characterisation • Phosphorylation • Intracellular trafficking • PDC deficiency • Genetic defects • Potential drug target

19.1 Introduction to Overall Complex Architecture, Macromolecular Organisation and the Reaction Cycle

Elucidation of the general architecture, subunit organisation and enzymology of bacterial and mammalian pyruvate dehydrogenase multi-enzyme complexes (PDCs) over the past 50 years has been achieved by a number of laboratories, including pioneering contributions from the groups of Lester Reed in Austin (Reed and Oliver 1982; Behal et al. 1989a, b; Reed et al. 1992); Richard Perham in Cambridge (Perham and Reche 1998; Perham et al. 1987); John Guest in Sheffield (Guest et al. 1989; Jordan et al. 1998) and Robert Harris in Indianapolis (Harris et al. 1997b, 2002; Popov et al. 1997). Each member of the 2-oxoacid dehydrogenase complex (2-OADC) family is composed of multiple copies of three distinct enzymes, termed E1, E2 and E3. Their overall morphology is determined by the central E2 enzyme that forms a pentagonal dodecahedral (60-meric) or cubic (24-meric) core acting as a framework to which multiple dimeric or hetero-tetrameric E1 and homo-dimeric E3 enzymes are tethered tightly, but non-covalently (Reed and Oliver 1982; Wagenknecht et al. 1990). In each case, these large central E2 assemblies are constructed from basic trimeric units that coalesce to form the 8 or 20 vertices of the E2 cube or dodecahedron, respectively. The 60-meric core is confined exclusively to PDCs from eukaryotic sources and Gram-positive bacteria. Interestingly, the E2 enzymes are all acyltransferases that are distantly related to chloramphenicol acetyltransferase, a naturally-occurring homo-trimer.

As shown in Fig. 19.1, the mammalian PDC reaction cycle involves the initial oxidative decarboxylation of pyruvate by its thiamine-diphosphate (ThDP)-requiring $\alpha_2\beta_2$ E1 enzyme, which also mediates transfer of the residual 2-carbon unit via an ethylidene-ThDP intermediate to reductively acetylate multiple lipoamide cofactors that are covalently linked to E2. Thereafter, E2 catalyses the transfer of the acetyl group to CoA, allowing the homodimeric dihydrolipoamide dehydrogenase (E3) to restore the reduced S_6, S_8 lipoamide thiols to their oxidised (disulphide) state, yielding acetyl CoA and NADH as final products.

19.1.1 E1, Pyruvate Dehydrogenase/Decarboxylase

E1 is a ThDP-dependent decarboxylase that catalyses the first, rate-limiting, irreversible step in the catalytic cycle (Cate et al. 1980; Berg et al. 1998). Initial decarboxylation of pyruvate is followed by the transfer of the ThDP-bound ethylidene

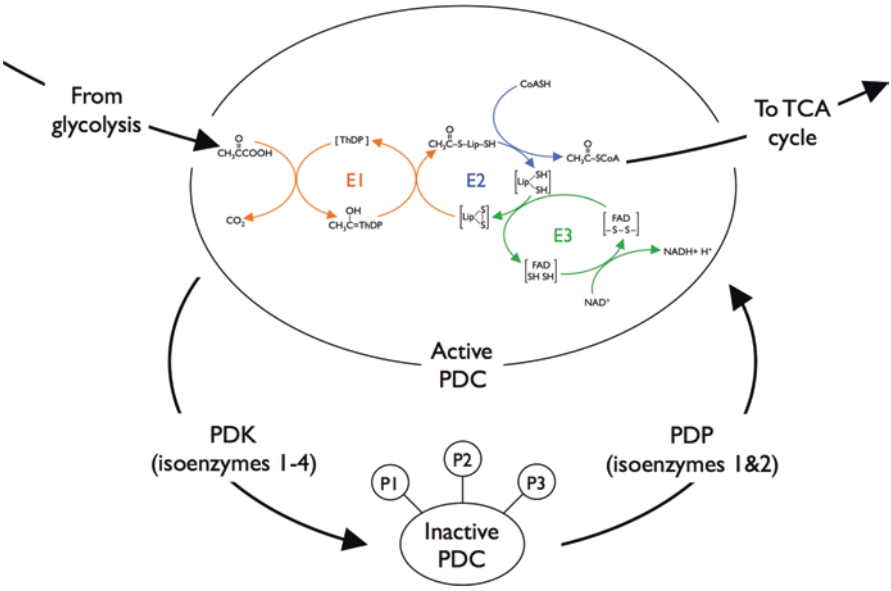

Fig. 19.1 PDC reaction cycle showing the active and inactive states of the multi-enzyme complex and the role of its associated kinases (PDK) and phosphatases (PDP) in its regulation by phosphorylation (P1-P3) and dephosphorylation of three specific serines in the E1α subunit

intermediate onto E2-linked lipoamide moieties in a reductive acetylation reaction. Both α_2 dimeric and $\alpha_2\beta_2$ tetrameric E1s house two active sites, each requiring Mg^{2+} ions and ThDP for activity. Several E1 crystal structures have been solved in recent years, including from *Escherichia coli* (Arjunan et al. 2002) and humans (Ciszak et al. 2003).

In the case of hetero-tetrameric E1s, the α and β subunits are related by a crystallographic two-fold axis of symmetry and arranged in a tetrahedral fashion. The active sites that bind ThDP are located in a 20 Å funnel-shaped tunnel formed at the α-β subunit interface, thereby facilitating access to the lipoyl-lysine moiety during the catalytic cycle. Hydrophobic contacts are primarily responsible for the stability of α/β subunit interactions. Biochemical, kinetic and spectral studies have demonstrated that E1 acts by a 'flip-flop' or alternating active-site mechanism. Thus, while one active site is participating in the pyruvate decarboxylation step, the other is simultaneously catalysing the reductive acetylation of an E2-lipoamide moiety (Yi et al. 1996; Sergienko et al. 2000; Sergienko and Jordan 2002; Kovina and Kochetov 1998; Khailova et al. 1990). X-ray structural studies have revealed that the ThDPs in the two E1 active sites communicate over a distance of 20 Å by reversibly shuttling a proton through an acidic tunnel in the protein. This proton 'wire' permits the cofactors to serve reciprocally as general acid/base catalysts and to switch the conformation of crucial active site peptide loops in a concerted manner (Frank et al. 2004).

Recently, an X-ray structure for a homo-dimeric E1:E2 di-domain (lipoyl domain (LD) plus subunit-binding domain (SBD), see below) sub-complex from *E. coli* has revealed a new folding motif located in the N-terminal region of E1 that is responsible for promoting a flexible and dynamic interaction with the E2 di-domain (Arjunan et al. 2014). This mode of interaction differs substantially in both location and nature from a previously-reported sub-complex of a SBD with an $\alpha_2\beta_2$ E1 from *Bacillus stearothermophilus* (Frank et al. 2005).

19.1.2 E2, Dihydrolipoamide Acetyltransferase

No high-resolution X-ray structures for any full-length E2-core assembly are available at present; however, crystal structures have been determined for both truncated 24- and 60-meric E2 constructs lacking their highly-mobile, modular N-terminal LDs and SBDs, as these are still capable of self-assembly (*Azotobacter vinelandii* (Mattevi et al. 1992); *B. stearothermophilus* (Milne et al. 2002); yeast (Stoops et al. 1992, 1997) and bovine PDC (Zhou et al. 2001b; Behal et al. 1994)). In both types, the fundamental building block is a basic trimeric unit, with 8 or 20 trimers associating to form a cube or pentagonal dodecahedron. Interestingly the inter-trimer contacts are much weaker than the intra-trimer ones, giving rise to a flexible, but well-connected core that is capable of 'breathing', a characteristic that may be essential for optimal PDC function by facilitating substrate channelling and active-site coupling (Zhou et al. 2001a; Kong et al. 2003).

High resolution cryo-EM reconstructions of human (Yu et al. 2008), bovine (Zhou et al. 2001b) and *Saccharomyces cerevisiae* (Stoops et al. 1992, 1997) cores as well as X-ray crystallographic structures of those from *Azotobacter vinelandii* (Mattevi et al. 1992, 1993) and *B. stearothermophilus* (Izard et al. 1999) have been determined. The C-terminal domains (CTDs) contain the conserved, active-site sequence motif, DHRXXDG, with the histidine and aspartate necessary for catalysis. The active-site is located in a 29 Å long channel that runs across the trimer at the CTD subunit interface. Interestingly, the two substrates that participate in the trans-acetylation reaction enter the active site from opposite directions. Coenzyme A enters from the interior of the hollow, highly-solvated core whereas the acetylated lipoamide moiety enters from the outside.

In recent years, the crystal structure of a unique 42-meric catalytic core of a 2-OADC from the thermophile *Thermoplasma acidophilum* has been solved at 4 Å resolution. In this structure the basic homo-trimeric units assemble into an oblate spheroid combining cubic and dodecahedral geometric elements (Marrott et al. 2012). Remarkably, the identical homo-trimeric building blocks of the 42-mer display differential modes of assembly, forming a polyhedral sphere with six pentagonal and three quadrilateral faces. In an extension of this study, removal of the five C-terminal amino acids of the E2 polypeptide (IIYEI) containing a key tyrosine involved in inter-trimer contacts results in the generation of a trimeric enzyme (Marrott et al. 2014). This minimal complex can bind both E1 and E3 components

to generate a branched-chain 2-oxoacid dehydrogenase complex with catalytic activity similar to the native multi-enzyme complex, raising the question as to why these assemblies are so large in nature. In this regard, it seems probable that the catalytic advantages conferred by their general ability to perform active-site coupling accounts for this phenomenon. Active-site coupling, first observed in *E. coli* PDC (Bates et al. 1977), involves the rapid transfer of acetyl groups from one lipoyl group to another around the entire surface of the core. Thus, the full complement of LDs can be acetylated from pyruvate entering via a single E1 enzyme. This remarkable cooperation of active sites provides a means of linking pyruvate and CoA, regardless of where they bind to the complex, ensuring enhanced rates of reaction even at low substrate concentrations (Marrott et al. 2014).

Central to the catalytic mechanism is the mobility of the N-terminally-located, E2-linked LDs that act as 'swinging arms', enabling their prosthetic groups to visit the active sites of all three enzymes during the catalytic cycle. This allows the lipoamide moieties to:

I. Be reductively acetylated by E1 (in the case of PDC)
II. Participate in E2-directed acetyl group transfer to CoA
III. Be returned to their oxidised state by reaction with E3 (Fig. 19.1)

The structural basis for these large-scale domain movements is the modular organisation of E2 that contains between one and three small N-terminal LDs (approximately 80 amino acids) separated by pro-ala-rich flexible linker regions of approximately 30 amino acids in length. These N-terminal domains extend outwards from the 24/60-meric core comprising the CTDs that are responsible for self-assembly and also house the acyltransferase active site. The overall LD structure is that of two four-stranded β-sheets forming a flattened β-barrel stabilised by a core of hydrophobic residues. The lipoamide prosthetic groups are bound to the ε-amino terminal of a key lysine residue situated at the exposed tip of a type 1 β-turn at one end of the domain with the N and C-termini close together at the opposite end on adjacent β-strands (Fig. 19.3a) (Howard et al. 1998). In this location, the dithiolane ring of the prosthetic group is itself situated approximately 14 Å above the surface of each LD as a result of its octanoate 'tail', allowing further extension of its reach and conformational flexibility (Perham 2000). A prominent conserved feature of LDs is a two-fold axis of quasi-symmetry relating the N and C-terminal halves of the domain (Dardel et al. 1993; Green et al. 1995; Ricaud et al. 1996).

NMR spectroscopy approaches have yielded vital insights into LD structure, dynamics and substrate specificity for their cognate E1/E3 enzymes and regulatory kinases (Kumaran et al. 2013). This approach has been aided significantly by the modular domain organisation of E2, the compact size of the LDs and SBDs and their ability to fold independently into functional entities. Moreover, the properties of linker regions that are rich in ala, pro and acidic amino acids have also been defined by NMR indicating that they have sufficient flexibility to account for the large-scale movements of the LDs during catalysis while retaining sufficient rigidity to ensure that they are held above the surface of the E2 core (Green et al. 1992). Mutational analysis has shown that the linker regions in *E. coli* PDC (approximately

30 amino acids) can be truncated by 50% before there is a significant effect on overall complex activity (Miles et al. 1988). In addition, peptide-specific hydrogen/deuterium mass spectrometry and NMR studies have been used to identify interaction loci on the E2/E3BP core with associated kinases (PDKs) 1 and 2 (Wang et al. 2015).

Enzymatic studies, using a series of E2 constructs containing multiple LDs, have also highlighted that the presence of 3 LDs per E2 chain is optimal in *E. coli* but that only the outermost domain need be lipoylated for maximal activity (Guest et al. 1997). Thus, the retention of 3 LDs in tandem repeat appears to be a mechanism for extending the reach of the outer domain prosthetic group rather than providing extra cofactors for catalysis. Interestingly, only a single LD is present on all members of the OGDC and BCOADC family that have an underlying 24-meric cubic core geometry in common with *E. coli* PDC.

19.1.3 E3, Dihydrolipoamide Dehydrogenase (E3)

Crystal structures of the FAD-containing E3 dimer have been solved from several prokaryotic and eukaryotic sources, namely *A. vinelandii* (Mattevi et al. 1991); *Pseudomonas fluorescens* (Mattevi et al. 1993); *B. stearothermophilus* (Mande et al. 1996); *S. cerevisiae* (Toyoda et al. 1998) and human (Brautigam et al. 2006). In all cases, E3 operates by a similar catalytic mechanism. In mammalian systems, E3 is a common component of all members of the 2-OADC family although complex-specific forms of E3 are found in some bacteria (Carothers et al. 1989; Burns et al. 1989). E3 catalyses the oxidation of the dihydrolipoamide prosthetic group on the LD of E2 via a 2-step 'ping-pong' mechanism. In the first step, electrons are transferred from reduced lipoamide via a reactive disulphide bridge to FAD, forming a stable intermediate complex. Subsequently, reducing equivalents are transferred to NAD^+ as the final electron acceptor. Despite a low sequence identity, the tertiary structures of prokaryotic and eukaryotic E3s are very similar. The E3 dimer is composed of identical subunits, each comprising 4 domains: an FAD domain, an NAD domain, a central domain and an interface domain. In the absence of FAD *in vitro*, the mammalian E3 polypeptide can fold to a significant extent, attaining a structure similar to its native state. However, it requires the presence of its FAD cofactor to promote the final conformational changes necessary for dimerisation and activation (Lindsay et al. 2000).

19.1.4 The Interaction of E1 and E3 with the Core Complex

Located between the CTD and LDs of E2 is a small and compact SBD, which, in 60-meric Gram-positive bacterial cores (e.g. *B. stearothermophilus*), serves to position E1 and E3 tightly with a 1:1 stoichiometry in a mutually exclusive manner, with

affinities in the nanomolar range (Mande et al. 1996). The E2-SBD binding sites on E1 and E3 are located across and close to the two-fold axis of symmetry, respectively (Frank et al. 2005). Occupation of both binding sites is prevented by steric clashes in one of the loop regions. In mammalian and yeast PDC, the equivalent domain has sole responsibility for promoting tight E1 interaction with the core. In these complexes, E3 is able to bind independently via an additional E2-related subunit referred to as E3 binding protein (E3BP). For many years E3BP was thought to be an E2 degradation product as it also contains an active LD; however, it was confirmed as an immunologically-distinct polypeptide in 1985 (De Marcucci and Lindsay 1985) and subsequently shown to be an integral, structural component of mammalian and yeast PDC responsible for E3 binding (Rahmatullah et al. 1989; Neagle and Lindsay 1991; Lawson et al. 1991). *In vitro* reconstitution of the E2 core lacking its E3BP partner confirmed the role of the latter subunit in high affinity E3 binding (McCartney et al. 1997).

The exact stoichiometry of E1 and E3 association with the SBDs of E2 and E3 remains unclear. While the crystal structure of the E3BP-SBD:E3 sub-complex suggests a 1:1 stoichiometry (Brautigam et al. 2006; Ciszak et al. 2006), solution structural studies have provided evidence for a 2:1 binding relationship (Smolle et al. 2006; Vijayakrishnan et al. 2011). In this model, E3 dimers (and possibly also E1 hetero-tetramers) have the potential to form 'cross-bridges' between adjacent E3BPs (and E2s) around the core surface (Vijayakrishnan et al. 2010). The presence of such 'cross-bridges' would provide a well-connected and robust network that may in turn promote enhanced movement and transfer of intermediates around the surface, thereby facilitating the efficiency of substrate channelling and active-site coupling.

19.1.5 Core Complex Heterogeneity

To date, it has not proved possible to crystallise any member of the 2-OADC family in its intact state. This is normally attributed to the size and complexity of these assemblies and in particular the high mobility of the E2-linked N-terminal lipoyl 'swinging arms' that are central to the multi-step catalytic mechanism. However, it is now apparent that the complexes also display intrinsic heterogeneity, so are not unique structures possessing a defined stoichiometry and subunit organisation. For example, in the PDC from *B. stearothermophilus*, the 60-meric E2 assembly can accommodate up to 60 E1 or 60 E3 enzymes that bind with similar affinities to overlapping, mutually-exclusive sites on E2 (Jung et al. 2002). Thus, the numbers and distribution of E1s and E3s around the core surface will vary from complex to complex and probably also in a time-dependent manner. In addition, there is the question of occupancy as there is no requirement to maintain saturation of all E1/E3 binding sites.

In eukaryotes, the structure and subunit composition of the E2/E3BP core is crucial for the efficient functioning of PDC. Initially, it was reported that 12E3BPs

were associated with the E2 core prompting the suggestion that individual E3 subunits were situated on the twelve pentagonal faces of the E2 icosahedral assembly-the so-called 'addition' model of core organisation (60E2 + 12E3BP) (Maeng et al. 1994, 1996; Sanderson et al. 1996). However, in subsequent 48E2+12E3BP and 40E2+20E3BP 'substitution' models, twelve or twenty E3BPs were proposed to replace an equivalent number of E2s within the 60-meric core assembly (Brautigam et al. 2009; Hiromasa et al. 2004). SAXS and SANS solution studies combined with cryo-EM reconstructions of recombinant human E2/E3BP cores reveal the presence of open pentagonal faces, strongly supporting the 'substitution' model (Vijayakrishnan et al. 2010) (Fig. 19.2). Variations in the reported subunit composition of the E2/E3BP core in the substitution model have been attributed to genuine differences between native and recombinant assemblies. In the latter case, a 40:20 E2/E3BP core is produced under defined conditions where E3BP is present in excess, suggesting that a single E3BP can be accommodated per trimer. In contrast, the native bovine E2/E3BP assembly has a 48:12 subunit stoichiometry. Mathematical modelling has predicted that an 'average' 48E2:12E3BP arrangement allows maximum flexibility in assembly while providing the appropriate balance of bound E1 and E3 enzymes for optimal catalytic efficiency and regulatory fine tuning (Vijayakrishnan et al. 2011).

In the case of eukaryotic PDCs where the central core 'scaffold' consists of two types of subunit, its overall composition is approximately 48E2:12E3BP (Vijayakrishnan et al. 2011); however, as discussed below, studies on recombinant E2/E3BP cores have shown that up to 20 E3BPs can substitute for 20 E2 subunits within the 60-meric structure suggesting that the composition of the native assembly may represent that of an 'average structure' derived from a heterogeneous population (Vijayakrishnan et al. 2011). It is also possible that the average subunit composition of the E2/E3BP 60-mer may vary from tissue to tissue as an additional means of fine tuning its activity to the prevailing metabolic conditions.

Despite these limitations, a variety of structural approaches have been employed successfully to gain new insights into the overall architecture and distinctive geometry of PDC and the molecular dynamics underlying its enzymatic processes. In most cases, high resolution X-ray structural data have been obtained for individual enzymes, e.g. the homo-dimeric E1 of *E. coli* (Arjunan et al. 2002)*;* the human $\alpha_2\beta_2$ E1 tetramer (Ciszak et al. 2003) and mammalian E3 (Brautigam et al. 2006). Truncated versions of the cubic and icosahedral E2 cores lacking their N-terminal LDs and SBDs have also proved amenable to crystallisation, providing detailed information on the E2 active-site geometry and the subunit contacts involved in oligomerisation in *Azotobacter vinelandii* (Mattevi et al. 1992, 1993)*; B. stearothermophilus* (Milne et al. 2002; Izard et al. 1999); yeast (Stoops et al. 1992, 1997) and bovine PDC (Zhou et al. 2001b; Behal et al. 1994). SAXS, SANS and AUC studies have further contributed to resolution between differing models of E2/E3BP core organisation and the modes of attachment of the peripheral E1 and E3 enzymes (Vijayakrishnan et al. 2010, 2011) (Fig. 19.2).

Over-expression in *E. coli*, purification and reconstitution of the component enzymes of human PDC has been successfully achieved in recent years although the

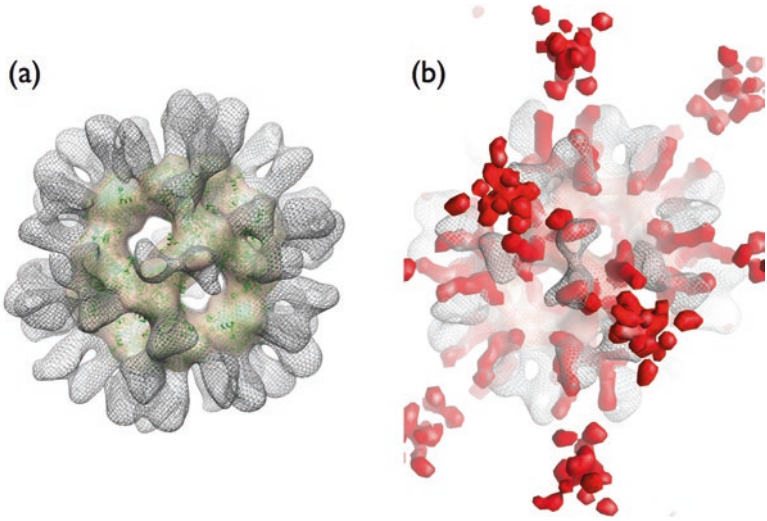

Fig. 19.2 Cryo-EM and SAXS models of recombinant human E2/E3BP and E2/E3BP:E3 complexes. (**a**) Cryo-EM reconstructions of the E2/E3BP (semi-transparent salmon-coloured surface) and E2/E3BP:E3 core (*grey mesh*), with the crystal structure of the *B. stearothermophilus* E2 core fitted within (*green ribbon*). The open faces of the core complex are easily visualised, consistent with the substitution model. (**b**) The E2/E3BP:E3 structure from (**a**) superimposed on the *ab initio* SAXS-derived E2/E3BP model (*red*). Extensions from the core surface consistent with SAXS data represent the LDs and SBDs not visualised by cryo-EM (Adapted with permission from Vijayakrishnan et al. 2010)

constituent subunits of both the $\alpha_2\beta_2$ E1 and E2/E3BP core enzymes must be co-expressed to promote their ordered integration and achieve the recovery of active enzyme (Korotchkina et al. 1995; Harris et al. 1997a). Reconstitution of fully-active recombinant human PDC is now a routine operation, as its three enzymes have an intrinsic capacity for self-association. Access to recombinant versions of the human complex is proving to be invaluable in the analysis of naturally-occurring and engineered mutations that provide new insights into the fundamental mechanisms of PDC function in health and disease (see below).

19.2 Biosynthesis and Assembly of Mammalian PDC

In common with the vast majority of mitochondrial polypeptides that are nuclear-encoded, the constituent subunits of mammalian PDC are synthesised on cytosolic ribosomes as individual precursor polypeptides containing an N-terminal targeting sequence that is recognised by specific receptors on the mitochondrial outer surface (Neupert 1997; Dudek et al. 2013; Becker et al. 2012). For matrix-located polypeptides, nascent chains are maintained in a loosely-folded, translocation competent state by cytoplasmic Hsp70 and Hsp90 chaperone complexes *en route* to the

organelle. They are then delivered to the mitochondrial matrix via the TOM 40 and TIM 23 (translocases of the outer and inner membranes) complexes located at specialised contact sites directing passage through the two membranes of the organelle. Translocation is facilitated by a matrix-located mitochondrial Hsp70 that transfers the nascent chains to the interior of the mitochondrial compartment. During this passage, their N-terminal extensions are removed by a pre-sequence processing protease situated on the interior aspect of the inner membrane. A matrix-located Hsp60/10 chaperone system, analogous to that found in bacteria, promotes the final maturation and assembly of the constituent enzymes of PDC prior to their rapid assembly into a mature, intact complex of over 200 polypeptides (Fox 2012; De Marcucci et al. 1988; Chacinska et al. 2009).

Remarkably, recent research has highlighted the possibility that the intact PDC can exit the mitochondrion and be transported *en bloc* to the nucleus in a cell cycle-dependent manner to provide a source of acetyl CoA for histone modification during S-phase (Sutendra et al. 2014; de Boer and Houten 2014). Although the validity of this research awaits independent confirmation, it raises the intriguing possibility that a novel pathway exists for nuclear-organelle communication and the export of mature, folded proteins and complexes. Potential candidates for this novel trafficking pathway are mitochondrial-derived vesicles (MDVs) for which a role in intracellular communication has been identified in recent years (Sugiura et al. (2014) and references therein). However, the size of these vesicles (70–100 Å) would appear to preclude their involvement in the transport of intact PDC (~450 Å), although partial disassembly of PDC into its component enzymes prior to transit is also a possibility (Sun et al. 2015; Soubannier et al. 2012; McLelland et al. 2014). Further work is essential to establish the authenticity of this novel mitochondrial export pathway or provide further insights into alternative mechanisms for translocation of mitochondrial polypeptides/complexes to various intracellular locations (Ng and Tang 2014).

19.3 Regulation of PDC by End-Product Inhibition and Phosphorylation

Control of PDC activity plays an important role in dictating the fuel used by various tissues in different nutritional and hormonal states. Thus, mammalian PDC is unusual amongst mitochondrial enzymes/complexes as, in addition to being subject to end-product inhibition by acetyl CoA and NADH, it is subject to control via its state of phosphorylation on a minute-by-minute basis. Fine control of PDC activity is of crucial importance in that it catalyses the key committed step in glucose utilisation, ensuring the appropriate balance between glucose or fatty acid and ketone body production. For example, it is down-regulated during starvation or diabetes in order to preserve carbohydrate reserves for tissues that are primarily dependent on

glucose for energy, whereas it is up-regulated after a meal to maximise energy production and fatty acid biosynthesis.

This acute or short-term regulation is primarily accomplished by four tightly-bound kinases (PDK1-4, related to bacterial histidine kinases (Fig. 19.1)) that are expressed in a tissue-specific manner at the level of one or two molecules per complex. Thus the phosphorylation state of PDC determines the flux of carbon through this vital committed step in carbohydrate metabolism since no net formation of glucose is possible from acetyl CoA. Collectively, this group of kinases targets one or more of three specific serine residues (site 1, Ser264; site 2, Ser271 and site 3, Ser203) on the E1α subunit with phosphorylation leading to complete inactivation in each case (Korotchkina and Patel 1995; Kolobova et al. 2001; Kato et al. 2008; Bao et al. 2004). PDK1 and 4 are highly expressed in heart, liver and muscle while PDK3 is prevalent in kidney, brain and testis and PDK2 is present in most tissues (Sugden and Holness 2003; Gudi et al. 1995; Bowker-Kinley et al. 1998). PDK1 phosphorylates all 3 serine residues in contrast to PDKs2–4 that can modify only sites 1 and 2 (Patel and Korotchkina 2001). Interestingly all four kinases modify these three serine residues at different rates and with different efficiencies, although phosphorylation at a single site is sufficient to cause inactivation, apparently by inhibiting substrate and/or ThDP binding in a site-specific manner (Korotchkina and Patel 2001). More specifically, an X-ray structure for a phosphorylated version of human E1 (site 1, Ser264) indicates that the phosphoryl group prevents ThDP-induced ordering of the two loops housing the three phosphorylation sites. These disordered loops impede binding of the LDs to E1, blocking their reductive acetylation and leading to disruption of substrate channelling (Kato et al. 2008).

PDKs1–3 are reported to interact with the E2 inner LD (ILD) while PDK4 binds to the E3BP-LD (Roche et al. 2003). PDK1-3 activity, in particular, is stimulated by their interaction with the E2-ILD and the lipoamide cofactor. Crystal structures of the ADP-bound form of the PDK2 and PDK3 dimers in association with the lipoylated E2-ILD have revealed in fine structural detail how their close association stimulates kinase activity. Conformational changes in the active-site clefts of both subunits result in disordering of the so-called ATP ‘lids’ in the ADP-bound state, thereby promoting rapid nucleotide release. Thus, structural and biochemical data suggest that E2-LD binding stimulates kinase activity by relieving end product inhibition (Kato et al. 2005; Green et al. 2008). A 2 Å resolution X-ray structure for PDK4 that normally binds the E3BP-LD, but is not significantly activated by this association, confirms this hypothesis. Its structure with bound ADP reveals an open conformation (in contrast to the closed conformation observed in the PDK2 and PDK3-ADP structures) in which there is a wide active-site cleft containing partially disordered C-terminal tails that facilitate the dissociation of bound nucleotide.

It is proposed that PDK4 with bound ADP exists in equilibrium between open and closed states with the favoured metastable open conformation being responsible for the robust basal activity of free PDK4 (Wynn et al. 2008). NADH, in addition to promoting end-product inhibition, is also able to enhance complex-bound kinase activity indirectly by altering the reduction/acetylation status of the lipoic acid prosthetic group on the E2/E3BP LDs. Recent H/D exchange mass spectrometry and

NMR studies have defined differences in the binding specificities and interaction loci of PDKs 1 and 2 for the two E2-linked LDs (Wang et al. 2015).

Reactivation of E1 is achieved by two specific heterodimeric phosphatases, PDPI and PDP2, comprising a catalytic and regulatory subunit allowing rapid fine tuning of PDC activity in response to prevailing metabolic conditions. PDP expression is also tissue-specific; PDP1 is mainly expressed in muscle whereas is PDP2 is abundant in liver and adipose tissue (Huang et al. 1998). PDP1, the dominant isoform, requires Mg^{2+} and is stimulated by micromolar levels of Ca^{2+} that are necessary to mediate binding to the E2-ILD (Damuni and Reed 1987). Pyruvate, acetyl CoA/CoA and NADH/NAD^+ ratios act as key effectors in feedback inhibition of PDC by influencing the redox and acetylation status of the lipoamide cofactors. While pyruvate inhibits PDK and acts as a positive inhibitor, NADH and acetyl CoA activate PDK and thereby act as negative regulators. A notable feature of the PDP1 crystal structure is a long insertion in the catalytic subunit creating a unique hydrophobic pocket capable of housing the lipoamide cofactor in a manner similar to that of PDKs, providing a structural basis for the indirect action of these effectors (Vassylyev and Symersky 2007).

Recent reports have also highlighted a novel mode of regulation of PDC activity, namely by control of its degree of lipoylation by SIRT4, a member of a family of seven mammalian NAD^+-dependent enzymes that govern diverse biological processes including genome regulation, stress responses and aging (Mathias et al. 2014). This ubiquitous group of enzymes, primarily known as lysine deacetylases, are involved in the removal of acetyl groups from key lysine residues, e.g. from histones during chromatin remodelling. However, evidence now suggests that several SIRTs can remove alternative lysine modifications such as succinyl and malonyl more efficiently than acetyl groups. Moreover, SIRTs 3–5 are mitochondrially-located while SIRTs 4 and 5 display little or no deacetylase activity. SIRT4 has now been shown to interact with E2-PDC where it promotes the efficient removal of lipoyl groups from the key lipoyl-lysines of the E2-LDs, diminishing PDC activity both *in vitro* and *in vivo* under appropriate metabolic conditions. The lipoamidase activity of SIRT4 may be a key factor in controlling the extent of lipoylation of all three members of the 2-OADC family, highlighting its central role as a guardian of cellular metabolism. Changes in lipoylation status will also impact on kinase and phosphatase regulation indirectly, given the importance of the lipoamide cofactor in mediating both kinase and phosphatase interactions with the complex.

19.4 Clinical Consequences of PDC Deficiency

The critical nature of the key metabolic step catalysed by the PDC implies that any loss-of-function mutations will be embryonic lethal. Moreover, specific natural mutations causing alterations in PDC activity were not readily identifiable until relatively recently in that the major indicator of PDC deficiency at the biochemical

level, metabolic acidosis, is a general hallmark of mitochondrial dysfunction (Brown et al. 1994). Neurodevelopmental delay, hypotonia and structural brain abnormalities typical of Leigh syndrome are the commonest clinical signs of PDC deficiency. Genetic lesions in all the constituent enzymes of PDC have now been identified (see Imbard et al. (2011) and Patel et al. (2012) for comprehensive reviews). In contrast, defects in the BCOADC give rise to maple syrup urine disease (MSUD) accompanied by elevated blood and urine levels of the branched-chain 2-oxoacids derived from leucine, isoleucine and valine that are also excreted giving rise to a characteristic sweet-smelling urine (Harper et al. 1990). All new-born infants are tested at birth for MSUD as exposure to high levels of these metabolites rapidly results in severe neurological and developmental problems. At present strict dietary control of branched-chain amino acid intake is the sole effective treatment for this genetic condition. Reports of genetic defects in OGDC are extremely rare, reflecting the central role of this complex in maintaining the integrity of the citric acid cycle (Gibson et al. 2012; Dumont et al. 2009).

Although complexes I and III of the mitochondrial respiratory chain are considered to be the primary generators of ROS in this organelle, PDC, OGDC and BCOADC are now recognised to be significant sources of superoxide/hydrogen peroxide production that can generate ROS at much higher rates than complex I (Quinlan et al. 2013, 2014; Tretter and Adam-Vizi 2005). Deficiencies in these complexes can also lead to increased oxidative stress via enhanced ROS generation. For example, induced mitochondrial dihydrolipoyl succinyltransferase (E2-OGDC) deficiency in a transgenic mouse model increases nitrotyrosine levels, amyloid plaque burden and results in the occurrence of spatial learning and memory defects. Thus, current evidence suggests that OGDC may be involved in the pathogenesis of Alzheimer's disease through increased oxidative stress (Dumont et al. 2009). Similarly, differences in phenotype and severity of symptoms in patients carrying specific mutations in these complexes may partly be accounted for by enhanced ROS generation in individual cases. A further complication is that PDKs (especially PDK2) are susceptible to inactivation by mitochondrial ROS, undermining the normal regulatory mechanisms governing PDC and BCOADC activity (Hurd et al. 2012).

19.5 Genetic Defects in PDC Deficient Patients: *In Vitro* Evaluation Using Recombinant Human PDC

As stated previously, a major advance in our understanding of PDC structure and function occurred in the 1980s and 1990s, initially from selective proteolysis and immunological studies on bovine PDC demonstrating that E3BP (originally called protein X) was an integral subunit of the complex that contributed to its overall function. Subsequent cloning and sequencing of genes encoding yeast and human E3BP revealed a high degree of sequence similarity to E2 although they lacked the

active site motif DHRXXDG essential for acetyltransferase activity (Harris et al. 1997a; Behal et al. 1989a). Disruption and mutagenesis of the *PDX1* gene encoding E3BP in yeast and studies of E3 binding to reassembled bovine E2 cores lacking E3BP confirmed the primary role of this subunit in high-affinity E3BP binding (McCartney et al. 1997; Lawson et al. 1991). In addition, immunoblotting of PDC subunits in cell and tissue samples from several patients with putative PDC deficiencies revealed a complete lack of the E3BP subunit while retaining partial PDC activity estimated at 10–20% of controls (Marsac et al. 1993). This residual activity has been attributed to the low-affinity binding of E3 to the E2 core even in the absence of E3BP (Singh 2008). Patients lacking any detectable E3BP protein are generally found to have deletions, nonsense mutations or point mutations at intron-exon boundaries that lead to aberrant splicing and prevent the production of a viable protein product (Brown et al. 2006; Aral et al. 1997).

In vitro reconstitution of the recombinant complex with recombinant E2/E3BP or E2 only core assemblies demonstrate that the native assembly becomes fully-activated with stoichiometric amounts of E3. Mutant PDC proved to be virtually inactive (3–5%) under these conditions; however, activity increased gradually to 40–50% of controls with a substantial excess of E3 (100-fold or greater (Singh 2008)). In contrast, a gradual decline in wild-type activity was observed at high E3 levels suggesting that E3 also interacts weakly with the E2-SBD and, at high concentrations, partially displaces the rate-limiting E1 enzyme. Surface plasmon resonance (SPR) data support this conclusion indicating that E3 binds to an E3BP-di-domain construct with a K_d of 5.3 ± 1.8 nM, whereas binding to the equivalent E2-di-domain was correspondingly weaker (80–100 fold) with a K_d of 0.4 ± 0.11 μM. This mutually exclusive binding is reminiscent of the situation in *B. stearothermophilus* PDC where E1 and E3 compete for an overlapping site on the E2 core.

Two unrelated cases of PDC deficiency linked to mutations in E2 have been described to date (Head et al. 2005). Of particular interest was the discovery of a patient with an unusual ‘in-frame’ 3-bp deletion encoding Glu121 of the mitochondrial precursor (Glu35 of the mature protein after removal of its 86 amino acid presequence prior to assembly). In this patient, who displayed relatively mild symptoms of PDC deficiency, activity was estimated at 25–35% of controls. As shown in Fig. 19.3c, Glu35 is situated in the central position of a small three-residue loop in the outer LD (OLD) joining β-strands 3 and 4. *In vitro* studies, employing recombinant wild-type and mutant LDs expressed as GST fusion proteins indicate that the ΔE121 deletion prevents its lipoylation and induces formation of LD dimers (Singh 2008). Reconstituted human PDC carrying the E35 deletion on the E2 OLD has 10–20% of overall complex activity, similar to patient values. In contrast, substitution of E35 with asp or gln, has no significant effect on the lipoylation status of the domain, does not induce dimerisation and has only minimal effects on the activity of reconstituted PDC (80–100% of controls). Biophysical studies (CD, tryptophan fluorescence spectroscopy and AUC) indicate that the presence of the ΔE121 OLD promotes large structural perturbations by interfering with the ordered, C-terminally-directed assembly of the E2/E3BP core as evidenced by the presence of multiple

non-specific aggregates. The increased tendency of these mutant OLDs to interact in an inappropriate fashion promoting dimer formation has a profound negative impact on normal E2/E3BP core formation (Fig. 19.3d) resulting in a disordered E2/E3BP core that is responsible for the symptoms of PDC deficiency in this patient.

Interestingly the removal of 2–4 residues from a prominent surface loop joining β-strands 1 and 2 of an *E. coli* LD (Fig. 19.3a) is also accompanied by an increasing tendency to form a novel misfolded dimer. Detailed NMR structural studies of this misfolded structure reveal that their N-terminal halves are unfolded and dynamic, causing the C-terminal halves of two monomers to associate forming a structure with twofold symmetry and a topology mimicking that of the folded monomer (Fig. 19.3b). In summary, surface loops, in particular their length, appear to be key determinants in the folding process that leads to normal LD formation (Stott et al. 2009).

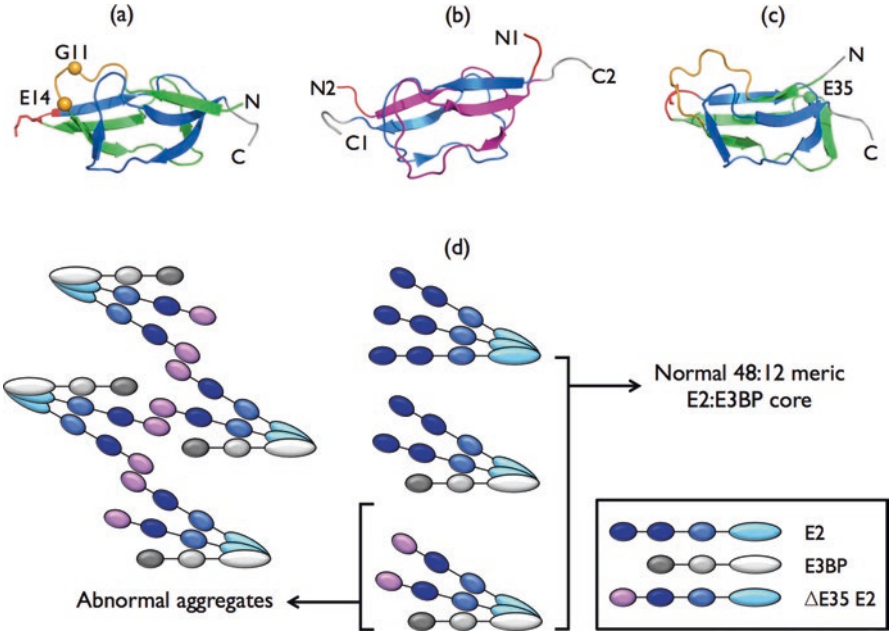

Fig. 19.3 Dimerisation of lipoyl domains induced by deletions in two key loop regions. (**a**) The NMR-derived structure of the ILD from *E. coli* (PDB ID: 1QJO, model 1) showing the position of selected residues (G11 to E14) within a prominent surface loop (*orange*) that when deleted result in the formation of dimers (**b**) as the result of mis-folding. At the core of the dimer (also observed via NMR spectroscopy (PDB ID: 2K7V)) are two β-sheets composed of the C-terminal halves (*blue* and *pink*) of two separate LDs. The unstructured N-terminal halves of the domains are not visualised here, for clarity (Stott et al. 2009). In (*c*) the position of E35 of the human ILD structure (PDB ID: 1FYC (Howard et al. 1998) in a different surface loop, is indicated since there is no structure for a human OLD. Deletion of this residue in recombinant human OLD also induces dimerisation of the domain (Singh 2008) as well as the formation of abnormal aggregates of the E2/E3BP core. The three residues that contain the lipoly-lysine are in red (*d*) trimers of E2 alone or which include one molecule of E3BP can then self-assemble to form normal (e.g. 48:12-meric) E2:E3BP core complex via interaction of the C-terminal domains. However, the ΔE35 (ΔE121 in the mitochondrial precursor) mutant tends to dimerise through its N-terminal domain, leading to the formation of abnormal aggregates

There is an old saying amongst biochemists and molecular biologists that ‘dead proteins tell no tales’ and indeed embarking on a site-directed mutagenesis programme with little or no knowledge of protein structure and mechanism of action can lead to difficulties in interpretation, often proving to be a rather fruitless and uninformative approach. However, recombinant PDC analysis of natural mutations in cases of PDC deficiency where there is always residual complex activity can provide detailed insights into the molecular basis of the disease (as in the above cases) while also contributing novel insights into enzyme mechanisms and mode of assembly.

19.6 PDC and the Major Diseases

In recent years, aberrant pyruvate metabolism linked to alterations in PDC activity, regulation and gene expression have been implicated in several of the major diseases currently affecting the human population (see Gray et al. (2014) for review and references therein). These include general neurodegenerative disorders such as Alzheimer’s disease and Parkinson’s disease, cancer (Saunier et al. 2016; Jeoung 2015), diabetes (Lee 2014; Jeoung 2015) and cardiovascular disease (Sun et al. 2015). In most cases, however, the aetiology of these progressive, long-term conditions and the direct involvement of PDC in particular is not well characterised so will not be discussed further at this stage. Instead the final section of this chapter will focus on three areas where there have been recent advances at the molecular level in highlighting a central role for PDC and its subunits, namely in the autoimmune condition, primary biliary cirrhosis (PBC), malarial parasite infection and multidrug resistance in bacteria.

19.6.1 Primary Biliary Cirrhosis (PBC)

Primary biliary cirrhosis (PBC) is a chronic, immune-mediated liver disease for which there is no cure and which can be halted only by liver transplant (itself no guarantee of escape from the disease). The bile duct damage associated with PBC is thought to arise from unique characteristics of biliary epithelial cell (BEC) apoptosis, wherein exposure of autoantigen to immune system effectors (Wang et al. 2014) causes lesions (Fig. 19.4). The autoantigens of PBC are E2 subunits of members of the 2-OADC family, chiefly PDC-E2. An anomaly in BEC apoptosis prevents S-glutathionylation-mediated degradation of PDC-E2 which is then exposed to autoimmune effector agents and itself becomes an autoantigen (Yamagiwa et al. 2014; Selmi et al. 2011). Eric Gershwin and colleagues have worked for many years to elucidate the etiology of this complex disease (Wang et al. 2014; Gershwin et al. 2000; Leung et al. 1996) and their findings, together with the work of others had strongly indicated that the major E2 epitope was the lipoamide moiety (including

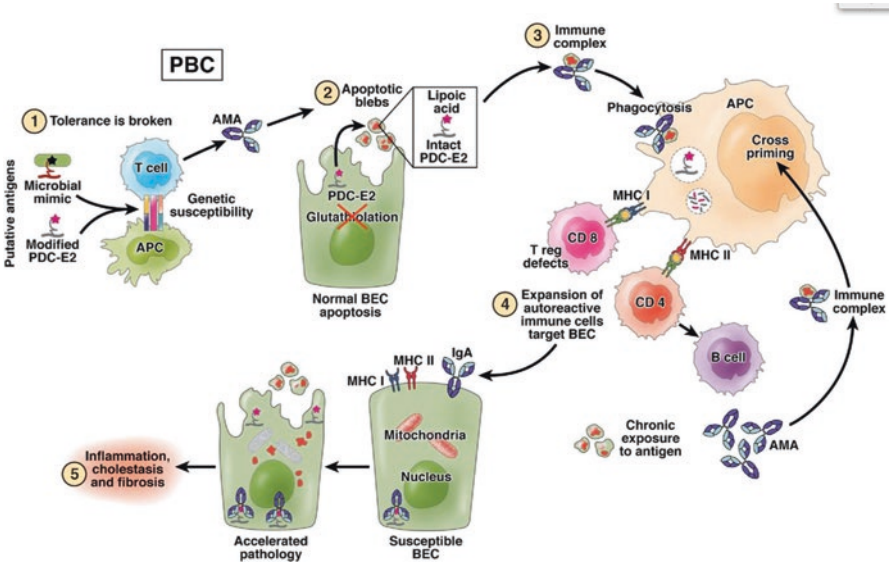

Fig. 19.4 The role of PDC in primary biliary cirrhosis (PBC). PBC is a complex, multi-factorial disease characterised by the loss of immune tolerance (1) to PDC E2, found in biliary epithelial cell (BEC) apoptotic blebs (2). Upon presentation of E2 to immune cells, immune complexes form (3), leading to the expansion of autoreactive immune cells (4) that target the BECs and cause chronic inflammation, cholestasis, and fibrosis (5). AMA, anti-mitochondrial antibody; APC, antigen-presenting cell; MHC, major histocompatibility complex. (Reproduced with permission from Hirschfield et al. 2010)

the lipoylated key lysine residue situated at the exposed type 1 β-turn tip) of the ILD.

The diagnosis of PBC relies on the indirect immunofluorescence detection of serum anti-mitochondrial antibodies (AMA, directed against PDC-E2) that are found in 95% of PBC cases. The AMA are tested using whole rat kidney tissue as the substrate but diagnosis could be better standardised if, instead, a panel of well-defined specific molecular targets was available. To this end Pacini et al. (2015) have developed a number of simple synthetic peptide antigens mimicking the main epitope on PDC-E2. In their work, solid-phase ELISA determination of the recognition of PBC patient sera by a panel of synthetic lipoylated and unlipoylated peptides, centred around the ILD key lysine (K173), revealed that lipoamide plays only a marginal role in IgM and IgG recognition. In order to understand the structural basis for this surprising finding, the structures of the synthetic peptides were determined by NMR spectroscopy, revealing a switch from random coil to helical conformation upon lipoylation. This modified, helical segment was then built into the existing NMR-derived structure for human unlipoylated (apo) PDC-E2 (PDB ID: 1FYC (Fig. 19.3c) (Howard et al. 1998)). After molecular dynamics (MD) simulations it was found that this helical region persisted, and owing to interactions of the lipoyl chain with proximal hydrophobic Leu and Ile side-chains in a groove formed

by strands 1 and 5 of the ILD, the lipoylated lysine becomes obscured and is thus less likely to form the PDC E2 ILD epitope (Selmi et al. 2011), the residual antigenicity of the lipoylated lysine observed arising from limited remaining conformational flexibility that may allow it to be occasionally accessible to antibody binding. Until an atomic resolution structure is determined for a lipoylated PDC-E2 ILD, it will not be possible to conclude whether this model does truly represent the positioning of the lipoyl group and whether its role in PBC requires re-evaluation.

19.6.2 Malaria

In the human malaria parasite *Plasmodium falciparum*, PDC is located exclusively in the apicoplast, a plastid-like organelle found in most apicomplexan parasites, where it provides acetyl-CoA for fatty acid biosynthesis and has no apparent function in providing acetyl-CoA for TCA activity (Jacot et al. 2016). Instead, *Plasmodium* uses its branched-chain 2-OADC complex to convert pyruvate to acetyl-CoA. *Plasmodium* PDC is essential for parasite survival in the mosquito vector and for late liver-stage development in the human host, suggesting its suitability as a target for intervention strategies against malaria. A study of *P. falciparum* apicoplast E3 (*Pf*aE3) used AUC, SAXS and discrete molecular dynamics (DMD) to demonstrate that two parasite-specific regions of the bacterially overexpressed recombinant protein extend from a dimeric compact core (Laine et al. 2015). In addition to the two extra loops, the high-resolution model consistent with the experimental AUC and SAXS data includes a two-stranded anti-parallel β motif in the space that, in the human E3 structure, is occupied by the E3BP SBD (Brautigam et al. 2006). Since the *P. falciparum* genome does not encode an *e3bp* homologue, *Pf*aE3 does not interact with E3BP SBD, but rather the SBD of *Pf*E2. If the presence of this hypothetical additional β motif could be experimentally confirmed (e.g. via MX) it would confirm the difference in this interaction from that observed for human E3-E3BP, supporting the suitability of *Pf*aE3 as a target for the development of intervention strategies. In addition to this, *Plasmodium* aE1α, aE1β and aE2 have been identified, through gene (protein and transcript) expression analysis studies, as three of several candidate genes for the generation of genetically attenuated parasites (GAPs) for use as live vaccines (Kumar et al. 2015). Because *Pf*aE2 lacks a human orthologue, it, like *Pf*aE3, might also make a good anti-malarial drug target.

19.6.3 Bacteria and Antimicrobials

It is known that certain bacteria, especially those with small genomes, double-up the function of some of their proteins such that glycolytic enzymes can be found on the bacterial surface interacting with host proteins. This has recently been demonstrated for two members of the genus *Mycoplasma*, namely *M. pneumoniae* and *M.*

agalactiae. Three PDC components (E1α, E1β and E2) have been found on the surface of *M. pneumoniae*. Additionally, in the presence of the serine kinase activator urokinase, *M. pneumoniae* PDC E1β was found to be capable of activating host plasminogen to plasmin and degrading fibrinogen (Gründel et al. 2015). The interaction between the PDC components and plasminogen is ascribed to the propensity of its five kringle domains to bind to lysine residues, in which bacterial proteins are especially rich. This work indicates that these surface-associated PDC components may play a role in *M. pneumoniae* virulence and is important in expanding our understanding of the process of human respiratory epithelium colonization by this pathogen. A mutant *M. agalactiae* defective in growth *in vitro* was generated by Hegde et al. (2015) via transposon mutagenesis insertion in the *pdhB* gene (which encodes PDC E1β). The mutant was observed to be far less effective in the invasion of HeLa cells but no less effective in cell adhesion (compared with the wild type strain) suggesting that although PDC E1β acts at a stage secondary to initial contact for internalisation into eukaryotic cells, it nonethless plays a significant role in infection by *M. agalactiae*. In neither report is the mechanism of PDC protein delivery to the bacterial cell surface investigated, nor the form in which the proteins are "displayed". Therefore it remains to be determined whether in *M. pneumoniae* E2 is present there as an oligomeric complex or as trimers or even monomers or whether E1β is within the E1 heterodimer, for instance.

Together with PDC E2 and E3, E1 is additionally reported to play a role in chemokine CXCL10-mediated antimicrobial activity in multidrug-resistant *E. coli* (Schutte et al. 2016). Sub-lethal concentrations of CXCL10 disrupt the ability of the *E. coli* to form long chains of cells. Transposon mutagenesis was once again used to identify the gene encoding *E. coli* PDC E1 as has being critical to the action of CXCL10, since the mutants were resistant to its antibacterial effects. Interestingly, generation of further mutants in E2 and E3 suggests that it is disruption of the PDC in its entirety that confers increased resistance to CXCL10-mediated killing. Immunogold-labelled CXCL10 located to the surface of *E. coli*, regardless of whether the gene for E1 had been disrupted or not, suggesting that the chemokine binds initially to something other than E1. Instead, the effect may be indirect and may arise from a subtle change in bacterial metabolism. For instance, the authors speculate that the mutant bacteria may resist CXCL10-mediated killing by directing energy production away from aerobic respiration and the TCA cycle and instead forcing it to proceed through other, less efficient, metabolic pathways. Since we face an era of increasing resistance to existing antibiotics, a better understanding of the mechanism by which CXCL10 exerts its antimicrobial effect may be an important step in the pathway to new drug targets for *E. coli* or other Gram-negative pathogens.

19.7 Outlook

Where next in our further understanding of the structural basis for the function of PDC and its related assemblies? Owing to its probable inherent heterogeneity, it is unlikely that an X-ray crystallographic structure for intact PDC will be determined. Instead, recent breath-taking advances in cryo-EM, delivering structures to 2.2 Å resolution (Doerr 2015), probably hold the key since this method can accommodate heterogeneity in structure and can capture the conformations of molecules and complexes whose flexibility evades structural study by MX. It has even become possible to determine (albeit lower-resolution) complex structures *in situ* (Engel et al. 2015), offering the tantalising possibility of direct observation of variations in PDC architecture from tissue to tissue and as a function of metabolic or disease state.

Acknowledgments The work of Swetha Vijayakrishnan and Geetanjali Singh that contributed to Figs. 19.2 and 19.3 of this chapter is gratefully acknowledged.

References

Aral B, Benelli C, Ait-Ghezala G, Amessou M, Fouque F, Maunoury C, Créau N, Kamoun P, Marsac C (1997) Mutations in *PDX1*, the human lipoyl-containing component X of the pyruvate dehydrogenase-complex gene on chromosome 11p1, in congenital lactic acidosis. Am J Hum Genet 61(6):1318–1326. doi:10.1086/301653

Arjunan P, Nemeria N, Brunskill A, Chandrasekhar K, Sax M, Yan Y, Jordan F, Guest JR, Furey W (2002) Structure of the pyruvate dehydrogenase multienzyme complex E1 component from *Escherichia coli* at 1.85 Å resolution. Biochemistry 41(16):5213–5221. doi:10.1021/bi0118557

Arjunan P, Wang J, Nemeria NS, Reynolds S, Brown I, Chandrasekhar K, Calero G, Jordan F, Furey W (2014) Novel binding motif and new flexibility revealed by structural analyses of a pyruvate dehydrogenase-dihydrolipoyl acetyltransferase subcomplex from the *Escherichia coli* pyruvate dehydrogenase multienzyme complex. J Biol Chem 289(43):30161–30176. doi:10.1074/jbc.M114.592915

Bao HY, Kasten SA, Yan XH, Roche TE (2004) Pyruvate dehydrogenase kinase isoform 2 activity limited and further inhibited by slowing down the rate of dissociation of ADP. Biochemistry 43(42):13432–13441. doi:10.1021/bi049488x

Bates DL, Danson MJ, Hale G, Hooper EA, Perham RN (1977) Self-assembly and catalytic activity of pyruvate dehydrogenase multienzyme complex of *Escherichia coli*. Nature 268(5618):313–316. doi:10.1038/268313a0

Becker T, Böttinger L, Pfanner N (2012) Mitochondrial protein import: from transport pathways to an integrated network. Trends Biochem Sci 37(3):85–91. doi:10.1016/j.tibs.2011.11.004

Behal RH, Browning KS, Hall TB, Reed LJ (1989a) Cloning and nucleotide-sequence of the gene for protein X from *Saccharomyces cerevisiae*. Proc Natl Acad Sci U S A 86(22):8732–8736. doi:10.1073/pnas.86.22.8732

Behal RH, Browning KS, Reed LJ (1989b) Nucleotide and deduced amino-acid sequence of the alpha-subunit of yeast pyruvate-dehydrogenase. Biochem Biophys Res Commun 164(2):941–946. doi:10.1016/0006-291x(89)91549-0

Behal RH, DeBuysere MS, Demeler B, Hansen JC, Olson MS (1994) Pyruvate dehydrogenase multienzyme complex – characterization of assembly intermediates by sedimentation velocity analysis. J Biol Chem 269(50):31372–31377

Berg A, Westphal AH, Bosma HJ, de Kok A (1998) Kinetics and specificity of reductive acylation of mild-type and mutated lipoyl domains of 2-oxo-acid dehydrogenase complexes from *Azotobacter vinelandii*. Eur J Biochem 252(1):45–50. doi:10.1046/j.1432-1327.1998.2520045.x

Bowker-Kinley MM, Davis WI, Wu PF, Harris RA, Popov KM (1998) Evidence for existence of tissue-specific regulation of the mammalian pyruvate dehydrogenase complex. Biochem J 329(1):191–196

Brautigam CA, Wynn RM, Chuang JL, Machius M, Tomchick DR, Chuang DT (2006) Structural insight into interactions between dihydrolipoamide dehydrogenase (E3) and E3 binding protein of human pyruvate dehydrogenase complex. Structure 14:611–621

Brautigam CA, Wynn RM, Chuang JL, Chuang DT (2009) Subunit and catalytic component stoichiometries of an *in vitro* reconstituted human pyruvate dehydrogenase complex. J Biol Chem 284(19):13086–13098. doi:10.1074/jbc.M806563200

Brown GK, Otero LJ, Le Gris M, Brown RM (1994) Pyruvate dehydrogenase deficiency. J Med Genet 31(11):875–879. doi:10.1136/jmg.31.11.875

Brown RM, Head RA, Morris AAM, Raiman JAJ, Walter JH, Whitehouse WP, Brown GK (2006) Pyruvate dehydrogenase E3 binding protein (protein X) deficiency. Dev Med Child Neurol 48(9):756–760. doi:10.1017/s0012162206001617

Burns G, Sykes PJ, Hatter K, Sokatch JR (1989) Isolation of a 3rd lipoamide dehydrogenase from *Pseudomonas putida*. J Bacteriol 171(2):665–668

Carothers DJ, Pons G, Patel MS (1989) Dihydrolipoamide dehydrogenase: functional similarities and divergent evolution of the pyridine nucleotide-disulfide oxidoreductases. Arch Biochem Biophys 268(2):409–425. doi:10.1016/0003-9861(89)90309-3

Cate RL, Roche TE, Davis LC (1980) Rapid intersite transfer of acetyl groups and movement of pyruvate dehydrogenase component in the kidney pyruvate dehydrogenase complex. J Biol Chem 255(16):7556–7562

Chacinska A, Koehler CM, Milenkovic D, Lithgow T, Pfanner N (2009) Importing mitochondrial proteins: machineries and mechanisms. Cell 138(4):628–644. doi:10.1016/j.cell.2009.08.005

Ciszak EM, Korotchkina LG, Dominiak PM, Sidhu S, Patel MS (2003) Structural basis for flip-flop action of thiamin pyrophosphate-dependent enzymes revealed by human pyruvate dehydrogenase. J Biol Chem 278(23):21240–21246. doi:10.1074/jbc.M300339200

Ciszak EM, Makal A, Hong YS, Vettaikkorumakankauv AK, Korochkina LG, Patel MS (2006) How dihydrolipoamide dehydrogenase-binding protein binds dihydrolipoamide dehydrogenase in the human pyruvate dehydrogenase complex. J Biol Chem 281:648–655

Damuni Z, Reed LJ (1987) Purification and characterization of a divalent cation-independent, spermine-stimulated protein phosphatase from bovine kidney mitochondria. J Biol Chem 262(11):5133–5138

Dardel F, Davis AL, Laue ED, Perham RN (1993) 3-dimensional structure of the lipoyl domain from *Bacillus stearothermophilus* pyruvate dehydrogenase multienzyme complex. J Mol Biol 229(4):1037–1048. doi:10.1006/jmbi.1993.1103

de Boer VCJ, Houten SM (2014) A mitochondrial expatriate: nuclear pyruvate dehydrogenase. Cell 158(1):9–10. doi:10.1016/j.cell.2014.06.018

De Marcucci O, Lindsay JG (1985) Component X - an immunologically distinct polypeptide associated with mammalian pyruvate-dehydrogenase multi-enzyme complex. Eur J Biochem 149(3):641–648. doi:10.1111/j.1432-1033.1985.tb08972.x

De Marcucci OGL, Gibb GM, Dick J, Lindsay JG (1988) Biosynthesis, import and processing of precursor polypeptides of mammalian mitochondrial pyruvate dehydrogenase complex. Biochem J 251(3):817–823

Doerr A (2015) Cryo-EM goes high-resolution. Nat Methods 12(7):598–599. doi:10.1038/nmeth.3469

Dudek J, Rehling P, van der Laan M (2013) Mitochondrial protein import: common principles and physiological networks. Biochimica Et Biophysica Acta-Mol Cell Res 1833(2):274–285. doi:10.1016/j.bbamcr.2012.05.028

Dumont M, Ho DJ, Calingasan NY, Xu H, Gibson G, Beal MF (2009) Mitochondrial dihydrolipoyl succinyltransferase deficiency accelerates amyloid pathology and memory deficit in a transgenic mouse model of amyloid deposition. Free Radic Biol Med 47(7):1019–1027. doi:10.1016/j.freeradbiomed.2009.07.008

Engel BD, Schaffer M, Albert S, Asano S, Plitzko JM, Baumeister W (2015) *In situ* structural analysis of Golgi intracisternal protein arrays. Proc Natl Acad Sci U S A 112(36):11264–11269. doi:10.1073/pnas.1515337112

Fox TD (2012) Mitochondrial protein synthesis, import and assembly. Genetics 192(4):1203–1234. doi:10.1534/genetics.112.141267

Frank RAW, Titman CM, Pratap JV, Luisi BF, Perham RN (2004) A molecular switch and proton wire synchronize the active sites in thiamine enzymes. Science 306(5697):872–876. doi:10.1126/science.1101030

Frank RAW, Pratap JV, Pei XY, Perham RN, Luisi BF (2005) The molecular origins of specificity in the assembly of a multienzyme complex. Structure 13(8):1119–1130. doi:10.1016/j.str.2005.04.021

Gershwin ME, Ansari AA, Mackay IR, Nakanuma Y, Nishio A, Rowley MJ, Coppel RL (2000) Primary biliary cirrhosis: an orchestrated immune response against epithelial cells. Immunol Rev 174:210–225

Gibson GE, Chen H-L, Xu H, Qiu L, Xu Z, Denton TT, Shi Q (2012) Deficits in the mitochondrial enzyme alpha-ketoglutarate dehydrogenase lead to Alzheimer's disease-like calcium dysregulation. Neurobiol Aging 33(6). doi:10.1016/j.neurobiolaging.2011.11.003

Gray LR, Tompkins SC, Taylor EB (2014) Regulation of pyruvate metabolism and human disease. Cell Mol Life Sci 71(14):2577–2604. doi:10.1007/s00018-013-1539-2

Green JDF, Perham RN, Ullrich SJ, Appella E (1992) Conformational studies of the interdomain linker peptides in the dihydrolipoyl acetyltransferase component of the pyruvate dehydrogenase multienzyme complex of *Escherichia coli*. J Biol Chem 267(33):23484–23488

Green JDF, Laue ED, Perham RN, Ali ST, Guest JR (1995) 3-dimensional structure of a lipoyl domain from the dihydrolipoyl acetyltransferase component of the pyruvate dehydrogenase multienzyme complex of *Escherichia coli*. J Mol Biol 248(2):328–343. doi:10.1006/jmbi.1995.0225

Green T, Grigorian A, Klyuyeva A, Tuganova A, Luo M, Popov KM (2008) Structural and functional insights into the molecular mechanisms responsible for the regulation of pyruvate dehydrogenase kinase 2. J Biol Chem 283(23):15789–15798. doi:10.1074/jbc.M800311200

Gründel A, Friedrich K, Pfeiffer M, Jacobs E, Dumke R (2015) Subunits of the pyruvate dehydrogenase cluster of *Mycoplasma pneumoniae* are surface-displayed proteins that bind and activate human plasminogen. PLoS One 10(5):e0126600. doi:10.1371/journal.pone.0126600

Gudi R, Bowker-Kinley MM, Kedishvili NY, Zhao Y, Popov KM (1995) Diversity of the pyruvate dehydrogenase kinase gene family in humans. J Biol Chem 270(48):28989–28994

Guest JR, Angier SJ, Russell GC (1989) Structure, expression, and protein engineering of the pyruvate dehydrogenase complex of *Escherichia coli*. Ann N Y Acad Sci 573:76–99. doi:10.1111/j.1749-6632.1989.tb14988.x

Guest JR, Attwood MM, Machado RS, Matqi KY, Shaw JE, Turner SL (1997) Enzymological and physiological consequences of restructuring the lipoyl domain content of the pyruvate dehydrogenase complex of *Escherichia coli*. Microbiology 143(2):457–466

Harper PAW, Healy PJ, Dennis JA (1990) Animal model of humandisease - maple syrup urine disease (branched-chain ketoaciduria). Am J Pathol 136(6):1445–1447

Harris RA, Bowker-Kinley MM, Wu PF, Jeng JJ, Popov KM (1997a) Dihydrolipoamide dehydrogenase-binding protein of the human pyruvate dehydrogenase complex – DNA-derived amino acid sequence, expression, and reconstitution of the pyruvate dehydrogenase complex. J Biol Chem 272(32):19746–19751. doi:10.1074/jbc.272.32.19746

Harris RA, Hawes JW, Popov KM, Zhao Y, Shimomura Y, Sato J, Jaskiewicz J, Hurley TD (1997b) Studies on the regulation of the mitochondrial alpha-ketoacid dehydrogenase complexes and

their kinases. In: Weber G (ed) Advances in Enzyme Regulation, vol 37, pp 271–293. doi:10.1016/s0065-2571(96)00009-x

Harris RA, Bowker-Kinley MM, Huang BL, Wu PF (2002) Regulation of the activity of the pyruvate dehydrogenase complex. In: Weber G (ed) Advances in Enzyme Regulation, vol 42, pp 249–259. doi:10.1016/s0065-2571(01)00061-9

Head RA, Brown RM, Zolkipli Z, Shahdadpuri R, King MD, Clayton PT, Brown GK (2005) Clinical and genetic spectrum of pyruvate dehydrogenase deficiency: dihydrolipoamide acetyltransferase (E2) deficiency. Ann Neurol 58(2):234–241. doi:10.1002/ana.20550

Hegde S, Rosengarten R, Chopra-Dewasthaly R (2015) Disruption of the *pdhB* pyruvate dehydrogenase gene affects colony morphology, *in vitro* growth and cell invasiveness of *Mycoplasma agalactiae*. PLOS One 10(6). doi:10.1371/journal.pone.0131134

Hiromasa Y, Fujisawa T, Aso Y, Roche E (2004) Organization of the cores of the mammalian pyruvate dehydrogenase complex formed by E2 and E2 plus the E3-binding protein and their capacities to bind the E1 and E3 components. J Biol Chem 279:6921–6933

Hirschfield GM, Heathcote EJ, Gershwin ME (2010) Pathogenesis of cholestatic liver disease and therapeutic approaches. Gastroenterology 139(5):1481–1496. doi:10.1053/j.gastro.2010.09.004

Howard MJ, Fuller C, Broadhurst RW, Perham RN, Tang JG, Quinn J, Diamond AG, Yeaman SJ (1998) Three-dimensional structure of the major autoantigen in primary biliary cirrhosis. Gastroenterology 115(1):139–146. doi:10.1016/s0016-5085(98)70375-0

Huang BL, Gudi R, Wu PF, Harris RA, Hamilton J, Popov KM (1998) Isoenzymes of pyruvate dehydrogenase phosphatase – DNA-derived amino acid sequences, expression, and regulation. J Biol Chem 273(28):17680–17688. doi:10.1074/jbc.273.28.17680

Hurd TR, Collins Y, Abakumova I, Chouchani ET, Baranowski B, Fearnley IM, Prime TA, Murphy MP, James AM (2012) Inactivation of pyruvate dehydrogenase kinase 2 by mitochondrial reactive oxygen species. J Biol Chem 287(42):35153–35160. doi:10.1074/jbc.M112.400002

Imbard A, Boutron A, Vequaud C, Zater M, de Lonlay P, Ogier de Baulny H, Barnerias C, Miné M, Marsac C, Saudubray J-M, Brivet M (2011) Molecular characterization of 82 patients with pyruvate dehydrogenase complex deficiency. Structural implications of novel amino acid substitutions in E1 protein. Mol Genet Metab 104(4):507–516. doi:10.1016/j.ymgme.2011.08.008

Izard T, Ævarsson A, Allen MD, Westphal AH, Perham RN, de Kok A, Hol WGJ (1999) Principles of quasi-equivalence and Euclidean geometry govern the assembly of cubic and dodecahedral cores of pyruvate dehydrogenase complexes. Proc Natl Acad Sci U S A 96(4):1240–1245. doi:10.1073/pnas.96.4.1240

Jacot D, Waller RF, Soldati-Favre D, MacPherson DA, MacRae JI (2016) Apicomplexan energy metabolism: carbon source promiscuity and the quiescence hyperbole. Trend Parasitol 32(1):56–70. doi:10.1016/j.pt.2015.09.001

Jeoung NH (2015) Pyruvate dehydrogenase kinases: therapeutic targets for diabetes and cancers. Diabetes Metab J 39(3):188–197. doi:10.4093/dmj.2015.39.3.188

Jordan F, Nemeria N, Guo FS, Baburina I, Gao YH, Kahyaoglu A, Li HJ, Wang J, Yi JZ, Guest JR, Furey W (1998) Regulation of thiamin diphosphate-dependent 2-oxo acid decarboxylases by substrate and thiamin diphosphate.Mg(II) - evidence for tertiary and quaternary interactions. Biochim Biophys Acta Protein Struct Mol Enzymol 1385(2):287–306. doi:10.1016/s0167-4838(98)00075-2

Jung HI, Bowden SJ, Cooper A, Perham RN (2002) Thermodynamic analysis of the binding of component enzymes in the assembly of the pyruvate dehydrogenase multienzyme complex of *Bacillus stearothermophilus*. Protein Sci 11(5):1091–1100. doi:10.1110/ps.4970102

Kato M, Chuang JL, Tso SC, Wynn RM, Chuang DT (2005) Crystal structure of pyruvate dehydrogenase kinase 3 bound to lipoyl domain 2 of human pyruvate dehydrogenase complex. EMBO J 24(10):1763–1774. doi:10.1038/sj.emboj.7600663

Kato M, Wynn RM, Chuang JL, Tso S-C, Machius M, Li J, Chuang DT (2008) Structural basis for inactivation of the human pyruvate dehydrogenase complex by phosphorylation: role of disordered phosphorylation loops. Structure 16(12):1849–1859. doi:10.1016/j.str.2008.10.010

Khailova L, Korochkina L, Severin S (1990) Intersite cooperativity in enzyme action of pyruvate dehydrogenase. In: Ju HB (ed) Biochemistry and Physiology of TDP Enzymes. VCH Weinheim, Blaubeuren, pp 251–261

Kolobova E, Tuganova A, Boulatnikov I, Popov KM (2001) Regulation of pyruvate dehydrogenase activity through phosphorylation at multiple sites. Biochem J 358:69–77. doi:10.1042/0264-6021:3580069

Kong YF, Ming DM, Wu YH, Stoops JK, Zhou ZH, Ma JP (2003) Conformational flexibility of pyruvate dehydrogenase complexes: a computational analysis by quantized elastic deformational model. J Mol Biol 330(1):129–135. doi:10.1016/s0022-2836(03)00555-2

Korotchkina LG, Patel MS (1995) Mutagenesis studies of the phosphorylation sites of recombinant human pyruvate dehydrogenase: site-specific regulation. J Biol Chem 270(24):14297–14304

Korotchkina LG, Patel MS (2001) Site specificity of four pyruvate dehydrogenase kinase isoenzymes toward the three phosphorylation sites of human pyruvate dehydrogenase. J Biol Chem 276(40):37223–37229. doi:10.1074/jbc.M103069200

Korotchkina LG, Tucker MM, Thekkumkara TJ, Madhusudhan KT, Pons G, Kim HJ, Patel MS (1995) Overexpression and characterization of human tetrameric pyruvate dehydrogenase and its individual subunits. Protein Expr Purif 6(1):79–90. doi:10.1006/prep.1995.1011

Kovina MV, Kochetov GA (1998) Cooperativity and flexibility of active sites in homodimeric transketolase. FEBS Lett 440(1–2):81–84. doi:10.1016/s0014-5793(98)01423-9

Kumar H, Frischknecht F, Mair GR, Gomes J (2015) *In silico* identification of genetically attenuated vaccine candidate genes for *Plasmodium* liver stage. Infect Genet Evol 36:72–81. doi:10.1016/j.meegid.2015.09.002

Kumaran S, Patel MS, Jordan F (2013) Nuclear magnetic resonance approaches in the study of 2-oxo acid dehydrogenase multienzyme complexes – a literature review. Molecules 18(10):11873–11903. doi:10.3390/molecules181011873

Laine M, Biddau M, Byron O, Müller S (2015) Biochemical and structural characterization of the apicoplast dihydrolipoamide dehydrogenase of *Plasmodium falciparum*. Biosci Rep 35(1). doi:10.1042/bsr20140150

Lawson JE, Behal RH, Reed LJ (1991) Disruption and mutagenesis of the *Saccharomyces cerevisiae* PDX1 gene encoding the protein X component of the pyruvate dehydrogenase complex. Biochemistry 30(11):2834–2839. doi:10.1021/bi00225a015

Lee I-K (2014) The role of pyruvate dehydrogenase kinase in diabetes and obesity. Diabetes Metab J 38(3):181–186. doi:10.4093/dmj.2014.38.3.181

Leung PSC, VandeWater J, Coppel RL, Nakanuma Y, Munoz S, Gershwin ME (1996) Molecular aspects and the pathological basis of primary biliary cirrhosis. J Autoimmun 9:119–128

Lindsay H, Beaumont E, Richards SD, Kelly SM, Sanderson SJ, Price NC, Lindsay JG (2000) FAD insertion is essential for attaining the assembly competence of the dihydrolipoamide dehydrogenase (E3) monomer from *Escherichia coli*. J Biol Chem 275(47):36665–36670. doi:10.1074/jbc.M004777200

Maeng CY, Yazdi MA, Niu XD, Lee HY, Reed LJ (1994) Expression, purification, and characterization of the dihydrolipoamide dehydrogenase-binding protein of the pyruvate dehydrogenase complex from *Saccharomyces cerevisiae*. Biochemistry 33(46):13801–13807. doi:10.1021/bi00250a034

Maeng CY, Yazdi MA, Reed LJ (1996) Stoichiometry of binding of mature and truncated forms of the dihydrolipoamide dehydrogenase-binding protein to the dihydrolipoamide acetyltransferase core of the pyruvate dehydrogenase complex from *Saccharomyces cerevisiae*. Biochemistry 35(18):5879–5882. doi:10.1021/bi9600254

Mande SS, Sarfaty S, Allen MD, Perham RN, Hol WGJ (1996) Protein-protein interactions in the pyruvate dehydrogenase multienzyme complex: dihydrolipoamide dehydrogenase complexed with the binding domain of dihydrolipoamide acetyltransferase. Structure 4(3):277–286. doi:10.1016/s0969-2126(96)00032-9

Marrott NL, Marshall JJT, Svergun DI, Crennell SJ, Hough DW, Danson MJ, van den Elsen JMH (2012) The catalytic core of an archaeal 2-oxoacid dehydrogenase multienzyme complex is a 42-mer protein assembly. FEBS J 279(5):713–723. doi:10.1111/j.1742-4658.2011.08461.x

Marrott NL, Marshall JJT, Svergun DI, Crennell SJ, Hough DW, van den Elsen JMH, Danson MJ (2014) Why are the 2-oxoacid dehydrogenase complexes so large? Generation of an active trimeric complex. Biochem J 463:405–412. doi:10.1042/bj20140359

Marsac C, Stansbie D, Bonne G, Cousin J, Jehenson P, Benelli C, Leroux J-P, Lindsay G (1993) Defect in the lipoyl-bearing protein-X subunit of the pyruvate-dehydrogenase complex in 2 patients with encephalomyelopathy. J Pediatr 123(6):915–920. doi:10.1016/s0022-3476(05)80387-7

Mathias RA, Greco TM, Oberstein A, Budayeva HG, Chakrabarti R, Rowland EA, Kang Y, Shenk T, Cristea IM (2014) Sirtuin 4 is a lipoamidase regulating pyruvate dehydrogenase complex activity. Cell 159(7):1615–1625. doi:10.1016/j.cell.2014.11.046

Mattevi A, Schierbeek AJ, Hol WGJ (1991) Refined crystal structure of lipoamide dehydrogenase from *Azotobacter vinelandii* at 2.2 Å resolution – a comparison with the structure of glutathione reductase. J Mol Biol 220(4):975–994. doi:10.1016/0022-2836(91)90367-f

Mattevi A, Obmolova G, Schulze E, Kalk KH, Westphal AH, de Kok A, Hol WGJ (1992) Atomic structure of the cubic core of the pyruvate dehydrogenase multienzyme complex. Science 255(5051):1544–1550. doi:10.1126/science.1549782

Mattevi A, Obmolova G, Kalk KH, Westphal AH, de Kok A, Hol WGJ (1993) Refined crystal structure of the catalytic domain of dihydrolipoyl transacetylase (E2p) from *Azotobacter vinelandii* at 2.6 Å resolution. J Mol Biol 230(4):1183–1199. doi:10.1006/jmbi.1993.1235

McCartney RG, Sanderson SJ, Lindsay JG (1997) Refolding and reconstitution studies on the transacetylase protein X (E2/X) subcomplex of the mammalian pyruvate dehydrogenase complex: evidence for specific binding of the dihydrolipoamide dehydrogenase component to sites on reassembled E2. Biochemistry 36(22):6819–6826. doi:10.1021/bi9630016

McLelland G-L, Soubannier V, Chen CX, McBride HM, Fon EA (2014) Parkin and PINK1 function in a vesicular trafficking pathway regulating mitochondrial quality control. EMBO J 33(4):282–295. doi:10.1002/embj.201385902

Miles JS, Guest JR, Radford SE, Perham RN (1988) Investigation of the mechanism of active site coupling in the pyruvate dehydrogenase multienzyme complex of *Escherichia coli* by protein engineering. J Mol Biol 202(1):97–106. doi:10.1016/0022-2836(88)90522-0

Milne JLS, Shi D, Rosenthal PB, Sunshine JS, Domingo GJ, Wu XW, Brooks BR, Perham RN, Henderson R, Subramaniam S (2002) Molecular architecture and mechanism of an icosahedral pyruvate dehydrogenase complex: a multifunctional catalytic machine. EMBO J 21(21):5587–5598. doi:10.1093/emboj/cdf574

Neagle JC, Lindsay JG (1991) Selective proteolysis of the protein X subunit of the bovine heart pyruvate dehydrogenase complex – effects on dihydrolipoamide dehydrogenase (E3) affinity and enzymatic properties of the complex. Biochem J 278:423–427

Neupert W (1997) Protein import into mitochondria. Annu Rev Biochem 66:863–917. doi:10.1146/annurev.biochem.66.1.863

Ng F, Tang BL (2014) Pyruvate dehydrogenase complex (PDC) export from the mitochondrial matrix. Mol Membr Biol 31(7–8):207–210. doi:10.3109/09687688.2014.987183

Pacini G, Carotenuto A, Rentier C, Nuti F, Real-Fernandez F, Brancaccio D, Sabatino G, Larregola M, Peroni E, Migliorini P, Novellino E, Battezzati PM, Selmi C, Papini AM, Rovero P (2015) Role of lipoylation of the immunodominant epitope of pyruvate dehydrogenase complex: toward a peptide-based diagnostic assay for primary biliary cirrhosis. J Med Chem 58(16):6619–6629. doi:10.1021/acs.jmedchem.5b00783

Patel MS, Korotchkina LG (2001) Regulation of mammalian pyruvate dehydrogenase complex by phosphorylation: complexity of multiple phosphorylation sites and kinases. Exp Mol Med 33(4):191–197

Patel KP, O'Brien TW, Subramony SH, Shuster J, Stacpoole PW (2012) The spectrum of pyruvate dehydrogenase complex deficiency: clinical, biochemical and genetic features in 371 patients. Mol Genet Metab 106(3):385–394

Perham RN (2000) Swinging arms and swinging domains in multifunctional enzymes: catalytic machines for multistep reactions. Annu Rev Biochem 69:961–1004. doi:10.1146/annurev.biochem.69.1.961

Perham RN, Reche PA (1998) Swinging arms in multifunctional enzymes and the specificity of post-translational modification. Biochem Soc Trans 26(3):299–303

Perham RN, Packman LC, Radford SE (1987) 2-oxo acid dehydrogenase multi-enzyme complexes: in the beginning and halfway there. Biochem Soc Symp 54:67–81

Popov KM, Hawes JW, Harris RA (1997) Mitochondrial alpha-ketoacid dehydrogenase kinases – a new family of protein kinases. In: Corbin JD, Francis SH (eds) Signal transduction in health and disease, Advances in second messenger and phosphoprotein research, vol 31. Lippincott-Raven, Philadelphia, pp 105–111

Quinlan CL, Perevoschikova IV, Goncalves RLS, Hey-Mogensen M, Brand MD (2013) The determination and analysis of site-specific rates of mitochondrial reactive oxygen species production. In: Cadenas E, Packer L (eds) Hydrogen peroxide and cell signaling, Pt A, Methods in Enzymology, vol 526. Academic, Amsterdam, pp 189–217. doi:10.1016/b978-0-12-405883-5.00012-0

Quinlan CL, Goncalves RLS, Hey-Mogensen M, Yadava N, Bunik VI, Brand MD (2014) The 2-oxoacid dehydrogenase complexes in mitochondria can produce superoxide/hydrogen peroxide at much higher rates than complex I. J Biol Chem 289(12):8312–8325. doi:10.1074/jbc.M113.545301

Rahmatullah M, Gopalakrishnan S, Andrews PC, Chang CL, Radke GA, Roche TE (1989) Subunit associations in the mammalian pyruvate-dehydrogenase complex – structure and role of protein X and the pyruvate dehydrogenase component binding domain of the dihydrolipoyl transacetylase component. J Biol Chem 264(4):2221–2227

Reed LJ, Oliver RM (1982) Structure-function-relationships in pyruvate and alpha-ketoglutarate dehydrogenase complexes. Adv Exp Med Biol 148:231–241

Reed LJ, Lawson JE, Niu XD, Yazdi MA, Fussey SP (1992) Biochemical and molecular genetic aspects of eukaryotic pyruvate dehydrogenase multienzyme complexes. J Nutr Sci Vitaminol (Tokyo) Spec No:46–51

Ricaud PM, Howard MJ, Roberts EL, Broadhurst RW, Perham RN (1996) Three-dimensional structure of the lipoyl domain from the dihydrolipoyl succinyltransferase component of the 2-oxoglutarate dehydrogenase multienzyme complex of *Escherichia coli*. J Mol Biol 264(1):179–190. doi:10.1006/jmbi.1996.0632

Roche TE, Hiromasa Y, Turkan A, Gong X, Peng T, Yan X, Kasten SA, Bao H, Dong J (2003) Essential roles of lipoyl domains in the activated function and control of pyruvate dehydrogenase kinases and phosphatase isoform 1. Eur J Biochem 270(6):1050–1056. doi:10.1046/j.1432-1033.2003.03468.x

Sanderson SJ, Miller C, Lindsay JG (1996) Stoichiometry, organisation and catalytic function of protein X of the pyruvate dehydrogenase complex from bovine heart. Eur J Biochem 236:68–77

Saunier E, Benelli C, Bortoli S (2016) The pyruvate dehydrogenase complex in cancer: an old metabolic gatekeeper regulated by new pathways and pharmacological agents. Int J Cancer 138(4):809–817. doi:10.1002/ijc.29564

Schutte KM, Fisher DJ, Burdick MD, Mehrad B, Mathers AJ, Mann BJ, Nakamoto RK, Hughes MA (2016) *Escherichia coli* pyruvate dehydrogenase complex is an important component of CXCL10-mediated antimicrobial activity. Infect Immun 84(1):320–328. doi:10.1128/iai.00552-15

Selmi C, Mackay IR, Gershwin ME (2011) The autoimmunity of primary biliary cirrhosis and the clonal selection theory. Immunol Cell Biol 89(1):70–80. doi:10.1038/icb.2010.126

Sergienko EA, Jordan F (2002) New model for activation of yeast pyruvate decarboxylase by substrate consistent with the alternating sites mechanism: demonstration of the existence of two active forms of the enzyme. Biochemistry 41(12):3952–3967. doi:10.1021/bi011860a

Sergienko EA, Wang J, Polovnikova L, Hasson MS, McLeish MJ, Kenyon GL, Jordan F (2000) Spectroscopic detection of transient thiamin diphosphate-bound intermediates on benzoylformate decarboxylase. Biochemistry 39(45):13862–13869. doi:10.1021/bi001214w

Singh G (2008) Analysis of genetic mutations using a recombinant model of the mammalian pyruvate dehydrogenase complex. PhD, University of Glasgow, Glasgow

Smolle M, Prior AE, Brown AE, Cooper A, Byron O, Lindsay JG (2006) A new level of architectural complexity in the human pyruvate dehydrogenase complex. J Biol Chem 281(28):19772–19780

Soubannier V, McLelland G-L, Zunino R, Braschi E, Rippstein P, Fon EA, McBride HM (2012) A vesicular transport pathway shuttles cargo from mitochondria to lysosomes. Curr Biol 22(2):135–141. doi:10.1016/j.cub.2011.11.057

Stoops JK, Baker TS, Schroeter JP, Kolodziej SJ, Niu XD, Reed LJ (1992) 3-dimensional structure of the truncated core of the *Saccharomyces cerevisiae* pyruvate dehydrogenase complex determined from negative stain and cryoelectron microscopy images. J Biol Chem 267(34):24769–24775

Stoops JK, Cheng RH, Yazdi MA, Maeng CY, Schroeter JP, Klueppelberg U, Kolodziej SJ, Baker TS, Reed LJ (1997) On the unique structural organization of the *Saccharomyces cerevisiae* pyruvate dehydrogenase complex. J Biol Chem 272:5757–5764

Stott KM, Yusof AM, Perham RN, Jones DD (2009) A surface loop directs conformational switching of a lipoyl domain between a folded and a novel misfolded structure. Structure 17(8):1117–1127. doi:10.1016/j.str.2009.07.001

Sugden MC, Holness MJ (2003) Recent advances in mechanisms regulating glucose oxidation at the level of the pyruvate dehydrogenase complex by PDKs. Am J Physiol Endocrinol Metab 284(5):E855–E862. doi:10.1152/ajpendo.00526.2002

Sugiura A, McLelland G-L, Fon EA, McBride HM (2014) A new pathway for mitochondrial quality control: mitochondrial-derived vesicles. EMBO J 33(19):2142–2156. doi:10.15252/embj.201488104

Sun W, Liu Q, Leng J, Zheng Y, Li J (2015) The role of pyruvate dehydrogenase complex in cardiovascular diseases. Life Sci 121:97–103. doi:10.1016/j.lfs.2014.11.030

Sutendra G, Kinnaird A, Dromparis P, Paulin R, Stenson TH, Haromy A, Hashimoto K, Zhang N, Flaim E, Michelakis ED (2014) A nuclear pyruvate dehydrogenase complex is important for the generation of acetyl-CoA and histone acetylation. Cell 158(1):84–97. doi:10.1016/j.cell.2014.04.046

Toyoda T, Suzuki K, Sekiguchi T, Reed LJ, Takenaka A (1998) Crystal structure of eukaryotic E3, lipoamide dehydrogenase from yeast. J Biochem (Tokyo) 123(4):668–674

Tretter L, Adam-Vizi V (2005) Alpha-ketoglutarate dehydrogenase: a target and generator of oxidative stress. Philos Trans Roy Soc B-Biol Sci 360(1464):2335–2345. doi:10.1098/rstb.2005.1764

Vassylyev DG, Symersky J (2007) Crystal structure of pyruvate dehydrogenase phosphatase 1 and its functional implications. J Mol Biol 370(3):417–426. doi:10.1016/j.jmb.2007.05.002

Vijayakrishnan S, Kelly SM, Gilbert RJC, Callow P, Bhella D, Forsyth T, Lindsay JG, Byron O (2010) Solution structure and characterisation of the human pyruvate dehydrogenase complex core assembly. J Mol Biol 399:71–93. doi:10.1016/j.jmb.2010.03.043

Vijayakrishnan S, Callow P, Nutley MA, McGow D, Gilbert D, Kropholler P, Cooper A, Byron O, Lindsay JG (2011) Variation in the organisation and subunit composition of the mammalian pyruvate dehydrogenase complex E2/E3BP core assembly. Biochem J 437(3):565–574

Wagenknecht T, Grassucci R, Schaak D (1990) Cryoelectron microscopy of frozen-hydrated alpha ketoacid dehydrogenase complexes from *Escherichia coli*. J Biol Chem 265(36):22402–22408

Wang L, Wang F-S, Chang C, Gershwin ME (2014) Breach of tolerance: primary biliary cirrhosis. Semin Liver Dis 34(3):297–317. doi:10.1055/s-0034-1383729

Wang J, Kumaran S, Zhou J, Nerneria NS, Tao H, Kakalis L, Park Y-H, Birkaya B, Patel MS, Jordan F (2015) Elucidation of the interaction loci of the human pyruvate dehydrogenase complex E2.E3BP core with pyruvate dehydrogenase kinase 1 and kinase 2 by H/D exchange mass spectrometry and nuclear magnetic resonance. Biochemistry 54(1):69–82. doi:10.1021/bi5013113

Wynn RM, Kato M, Chuang JL, Tso S-C, Li J, Chuang DT (2008) Pyruvate dehydrogenase kinase-4 structures reveal a metastable open conformation fostering robust core-free basal activity. J Biol Chem 283(37):25305–25315. doi:10.1074/jbc.M802249200

Yamagiwa S, Kamimura H, Takamura M, Aoyagi Y (2014) Autoantibodies in primary biliary cirrhosis: recent progress in research on the pathogenetic and clinical significance. World J Gastroenterol 20(10):2606–2612. doi:10.3748/wjg.v20.i10.2606

Yi JZ, Nemeria N, McNally A, Jordan F, Machado RS, Guest JR (1996) Effect of substitutions in the thiamin diphosphate-magnesium fold on the activation of the pyruvate dehydrogenase complex from *Escherichia coli* by cofactors and substrate. J Biol Chem 271(52):33192–33200

Yu X, Hiromasa Y, Tsen H, Stoops JK, Roche TE, Zhou ZH (2008) Structures of the human pyruvate dehydrogenase complex cores: a highly conserved catalytic center with flexible N-terminal domains. Structure 16(1):104–114. doi:10.1016/j.str.2007.10.024

Zhou ZH, Liao WC, Cheng RH, Lawson JE, McCarthy DB, Reed LJ, Stoops JK (2001a) Direct evidence for the size and conformational variability of the pyruvate dehydrogenase complex revealed by three-dimensional electron microscopy – the "breathing" core and its functional relationship to protein dynamics. J Biol Chem 276(24):21704–21713. doi:10.1074/jbc.M101765200

Zhou ZH, McCarthy DB, O'Connor CM, Reed LJ, Stoops JK (2001b) The remarkable structural and functional organization of the eukaryotic pyruvate dehydrogenase complexes. Proc Natl Acad Sci U S A 98(26):14802–14807. doi:10.1073/pnas.011597698